

High-Pressure Structural Phase Transitions in Na, Mg, and Al

John A. Moriarty and A. K. McMahan

Lawrence Livermore National Laboratory, University of California, Livermore, California 94550

(Received 23 December 1981)

First-principles total-energy calculations by two independent methods predict new transition-metal-like sequences of stable crystal structures in the third-period simple metals Na, Mg, and Al, under increasing pressure. These structural phase transitions are controlled by d electrons through the lowering and partial filling of the initially empty $3d$ band as the metals are compressed. A number of these transitions occur in the megabar range and below and could be investigated by existing experimental techniques.

PACS numbers: 64.70.Kb, 61.50.Lt, 62.50.+p

There has been a rapidly growing interest in understanding the systematics of crystal phase stability in elemental metals¹⁻¹⁰ and their binary compounds.^{11,12} For nonsimple metals, a recurring theme in most,^{3-9,11} although not all,^{10,12} of this work is the critical role played by the d electrons in explaining many of the observed trends. We present here theoretical evidence that under sufficiently high pressure the controlling influence of d electrons on crystal structure is extended to even simple metals and we predict new, as yet undetected, structural phase transitions in the third-period metals Na, Mg, and Al. Specifically, we have performed a series of first-principles total-energy calculations which suggest the possible sequence of structures hcp \rightarrow bcc \rightarrow hcp in Na, hcp \rightarrow bcc \rightarrow fcc in Mg, and fcc \rightarrow hcp \rightarrow bcc in Al under increasing pressure. These sequences are similar to those observed in transition-series metals with increasing atomic number and, at least for Mg and Al, result from the lowering and partial filling of the initially unoccupied $3d$ band as the metals are compressed. In addition, for Mg and Al we have obtained the same qualitative results from two entirely different techniques: the generalized pseudopotential theory (GPT)⁶ and the linear-muffin-tin-orbitals (LMTO) method.¹³

With both the GPT and LMTO methods, our analysis is based on calculation of the zero-temperature total energy of the solid as a function of atomic volume and crystal structure,¹⁴ within the general framework of the Kohn-Sham local-density formalism,¹⁵ using the Hedin-Lundqvist prescription for exchange and correlation.¹⁶ Beyond that common starting point, however, the two methods utilize quite different secondary approximations. In the GPT, all three metals are treated in the simple-metal limit of the theory, which represents a refined version of the conventional nonlocal pseudopotential perturba-

tion theory.^{1,6} A rigorous, optimized pseudo-potential of the orthogonalized-plane-wave type is employed. The two important approximations in this case are the small-core treatment of the inner-core electrons ($1s$, $2s$, and $2p$ here) and the neglect of third- and higher-order (structure-dependent) terms in the total energy expansion. In the LMTO method, on the other hand, we employ the atomic-sphere approximation (ASA),¹³ in which the electron density is spherically averaged within the Wigner-Seitz spheres. The LMTO method effectively retains the higher-order terms discarded in the GPT, but at the same time introduces the structure-dependent ASA which the GPT does not. Except as indicated, the present LMTO calculations were carried out as described in previous work on silicon,¹⁷ with *all* electrons treated self-consistently and s , p , and d components retained in the angular momentum basis. The LMTO structural energy differences are insensitive, over the volume range considered, to whether the $2s$ and $2p$ states are treated as bands or as atomic levels, indicating that the GPT small-core approximation for these electrons is adequate.

Total-energy calculations with use of the GPT and the LMTO methods have been carried out for fcc, bcc, and (ideal) hcp structures, over a range in atomic volume Ω extending from normal density ($\Omega = \Omega_0$) down to the vicinity of tenfold compression ($\Omega/\Omega_0 = 0.1$). The resultant structural energy differences, relative to the fcc phase, are plotted in Figs. 1 and 2. Figures 1(a) and 1(b) show our GPT results for Na and Mg, respectively, while Figs. 2(a) and 2(b) give a direct comparison of our LMTO and GPT results for Al. As can be seen in Fig. 2, the qualitative agreement between GPT and LMTO predictions about phase stability in Al is excellent: Both show large regions of fcc stability near normal volume and bcc stability at high compression

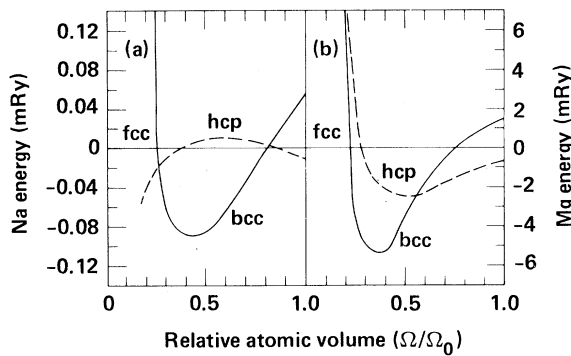


FIG. 1. Relative total energies of bcc, hcp, and fcc structures vs volume, as calculated by the GPT method. (a) Na and (b) Mg.

separated by a small island of hcp stability. The qualitative agreement for Mg is comparable. No LMTO calculations on Na were attempted because of the tiny energy differences (typically <0.1 mRy) between phases in that metal.

The structural energy differences in Mg and Al are profoundly influenced at high densities by the presence of d electrons. Under compression, the initially empty $3d$ band moves downward towards the Fermi level E_F , narrowing relative to the sp bands in the process. In Al, the LMTO X_3 level (approximately the bottom of the $3d$ band) moves below E_F at $\Omega/\Omega_0 = 0.15$, at which point each Wigner-Seitz cell contains about one d electron. We have directly assessed the effect of this d charge by repeating the LMTO calculations with d components removed from the angular momentum basis. The effect is striking, as shown in Fig. 3 for Al. The resultant bcc-fcc and hcp-fcc total energy differences now remain positive throughout the whole volume range considered. Analogous behavior is found for Mg. Thus *without d electrons Mg and Al would remain hcp and fcc, respectively, down to at least $\Omega/\Omega_0 = 0.1$.* Moreover, the *addition* of f components to the basis changes the results in Figs. 2(a) and 3 only slightly.

The increasing quantitative discrepancies between GPT and LMTO results with decreasing volume, as seen in Figs. 2 and 3, are probably due to differing treatments of d states. While the LMTO method is presumably treating the d states accurately regardless of their spatial character (i.e., either nearly-free-electron or tight-binding like), the GPT, as applied here in the simple-metal limit, is treating the d states accurately only to the extent that they remain nearly-free-electron like. Indeed, the purely

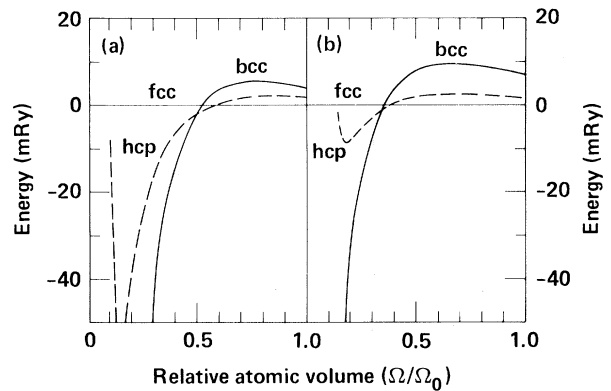


FIG. 2. Relative total energies of the bcc, hcp, and fcc structures of Al vs volume, as calculated by (a) the LMTO methods, and (b) the GPT method.

p -like X_4 , and L_2 , levels are calculated to within a few percent of each other by the two techniques at all volumes. The sd hybridized X_1 level, on the other hand, shows close agreement only near normal volume, with the LMTO value moving progressively lower than the GPT value upon compression. This lowering is exactly the type

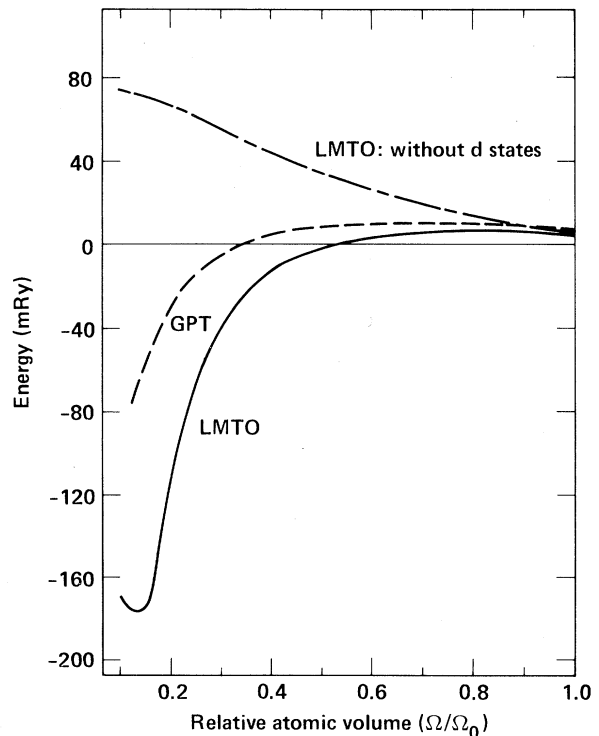


FIG. 3. The bcc-fcc total energy difference for Al vs volume, as calculated by the GPT method and by the LMTO method with and without d states.

of hybridization effect one expects from a narrowed d band centered above E_F and suggests that the $3d$ band in Al is slowly developing some tight-binding-like character under pressure, which the present simple-metal form of the GPT is not detecting. The natural remedy to this situation is to treat Al as an empty- d -band metal in the manner of the heavy alkali and alkaline-earth metals.⁶ This possibility is currently under study.

At lower densities it is possible that the ASA in the LMTO method is most responsible for quantitative differences between our GPT and LMTO results. At normal density both methods correctly identify the observed stable structure in each case and the calculated hcp-fcc energy differences are in good quantitative agreement. The GPT energy differences involving the bcc structure, however, are always larger and generally in better agreement with the available experimental data than the corresponding LMTO values, as shown in Table I. This is consistent with the expectation that spherical averaging inherent in the ASA should be better for the close-packed structures than for the more open bcc structure.

An interesting common feature of our results is a predicted region of bcc stability in all three metals under pressure. This is reminiscent of

the occurrence of the bcc phase in the center of the transition metals, which has been ascribed to the half filling of a narrow d band.^{3,4} The true origin of our bcc stability, however, appears to be more subtle. For example, the point of greatest bcc stability in Al ($\Omega/\Omega_0 \sim 0.15$ for our LMTO calculation) corresponds to only a 10% filling of the $3d$ band. Moreover, the effect of d -band occupation is generally opposite in Al and Mg, tending to stabilize the bcc structure in Al, while destabilizing that structure in Mg near $\Omega/\Omega_0 = 0.15$. We have analyzed this situation in detail and believe it can be understood from the one-electron density of states. As suggested by Andersen's force relation,⁴ we find the structural energy differences within the ASA well approximated by just the difference in (occupied) one-electron eigenvalue sums, provided the *same* potential is used for each lattice structure. We have calculated LMTO eigenvalue sums for Mg and Al, using the respective convergent fcc potentials for $\Omega/\Omega_0 = 0.15$. For *both* the Mg and Al sums, we find fcc stability for two-electron occupation (i.e., Mg) and bcc stability for three-electron occupation (i.e., Al). The former occurs because the lowering of the $3d$ band causes semi-metal behavior near $\Omega/\Omega_0 = 0.15$, creating a large dip in the fcc density of states at the two-electron E_F , in exactly the manner reported for fcc Ca at larger volumes.²¹ Neither the bcc nor hcp structures have such dips in their density of states. Relative to these structures, therefore, the fcc structure has state density shifted away from the two-electron E_F down to lower energies, giving it the lowest eigenvalue sum. Since the dip in the fcc density of states also implies state density shifted to higher energies above the two-electron E_F , this same argument would make the fcc structure unfavorable if another valence electron were added. This is precisely what happens for Al.

Lastly, we estimate the initial hcp - bcc transitions in Na and Mg, and fcc - hcp transition in Al, to occur at pressures of about 10, 570, and 1300 kbar at zero temperature, corresponding to $\Omega/\Omega_0 = 0.86, 0.56, \text{ and } 0.58$, respectively.¹⁴ While Na is complicated by a temperature-induced hcp - bcc transition at 36 K and ambient pressure,¹⁸ high-pressure bcc stability has been observed at 77 K up to 600 kbar.²² There is also evidence at room temperature of anomalous behavior in Mg near 100 kbar,²³ and possibly a partial fcc-to-hcp transition in Al at about 205 kbar.²⁴ Since high-pressure technology has improved dramatically in recent years, new experimental investigation

TABLE I. Normal density structural energy differences for Na, Mg, and Al as calculated by the GPT and the LMTO methods, and compared with available experimental data. Energy differences are in millirydbergs.

	bcc-fcc	hcp-fcc	bcc-hcp
Na			
GPT	0.055	-0.010	0.065
Expt.			0.055 ^a
Mg			
LMTO	0.2	-0.7	0.9
GPT	1.5	-0.6	2.1
Expt.	2.0 ^b	-1.5 ^b	3.5 ^b
Al			
LMTO	3.9	1.9	2.0
GPT	7.3	1.9	5.4
Expt.	7.7 ^b	4.2 ^b	3.5 ^b

^a Measured heat of transformation (0.032, Ref. 18) less the calculated bcc-hcp difference in zero-point vibrational energies (-0.023, Ref. 19).

^b Thermodynamically based estimates of Ref. 20.

of all three elements would be of considerable interest.

This work was performed under the auspices of the U. S. Department of Energy by Lawrence Livermore National Laboratory under Contract No. W-7405-Eng.-48.

¹V. Heine and D. Weaire, *Solid State Phys.* **24**, 249 (1970); W. A. Harrison, *Pseudopotentials in the Theory of Metals* (Benjamin, New York, 1966).

²C. Friedli and N. W. Ashcroft, *Phys. Rev. B* **12**, 5552 (1975).

³D. G. Pettifor, *J. Phys. C* **3**, 367 (1970), and references therein.

⁴A. R. Mackintosh and O. K. Andersen, in *Electrons at the Fermi Surface*, edited by M. Springford (Cambridge Univ. Press, New York, 1980), p. 149. The force relation is discussed on pp. 187, 188, and 192.

⁵J. A. Moriarty, *Phys. Rev. B* **8**, 1338 (1973).

⁶J. A. Moriarty, *Phys. Rev. B* **10**, 3075 (1974), and **16**, 2537 (1977), and to be published.

⁷B. Johansson and A. Rosengren, *Phys. Rev. B* **11**, 2836 (1975).

⁸J. C. Duthie and D. G. Pettifor, *Phys. Rev. Lett.* **38**, 564 (1977).

⁹Y. K. Vohra, H. Olijnik, W. Grosshans, and W. B. Holzapfel, *Phys. Rev. Lett.* **47**, 1065 (1981).

¹⁰S. Alexander and J. McTague, *Phys. Rev. Lett.* **41**, 702 (1978).

¹¹E. S. Machlin and B. Loh, *Phys. Rev. Lett.* **45**, 1642 (1980), and **47**, 1087 (1981).

¹²A. Zunger, *Phys. Rev. Lett.* **44**, 582 (1980), and *Phys. Rev. B* **22**, 5839 (1980), and *Phys. Rev. Lett.* **47**, 1086 (1981).

¹³O. K. Andersen, *Phys. Rev. B* **12**, 3060 (1975); O. K. Andersen and O. Jepsen, *Physica (Utrecht)* **91B**, 317 (1977).

¹⁴In the present work, we find the Gibbs free-energy differences between phases to be essentially identical to the total energy differences. (See also Ref. 5.)

Zero-point vibrational contributions have also not been included in our primary results, since GPT calculations show that they have negligible effect on the structural energy differences for Mg and Al. However, they do eliminate the tiny pocket of fcc stability seen in Fig. 1(a) for Na, causing the bcc energy to drop below the hcp energy at $\Omega/\Omega_0 = 0.86$.

¹⁵W. Kohn and L. J. Sham, *Phys. Rev.* **140**, A1133 (1965).

¹⁶L. Hedin and B. I. Lundqvist, *J. Phys. C* **4**, 2064 (1971). The LMTO calculations actually used the correlation potential of U. von Barth and L. Hedin, *J. Phys. C* **5**, 1629 (1972), but test calculations showed this to be an insignificant difference.

¹⁷A. K. McMahan, M. T. Yin, and M. L. Cohen, *Phys. Rev. B* **24**, 7210 (1981). The Ewald correction discussed therein has negligible effect on the present structural energy differences, and is omitted.

¹⁸D. L. Martin, *Proc. Roy. Soc. London, Ser. A* **254**, 433 (1960).

¹⁹G. K. Straub and G. C. Wallace, *Phys. Rev. B* **3**, 1234 (1971).

²⁰L. Kaufman and H. Bernstein, *Computer Calculation of Phase Diagrams* (Academic, New York, 1970).

²¹J.-P. Jan and H. L. Skriver, *J. Phys. F* **11**, 805 (1981).

²²R. Stager and H. G. Drickamer, *Phys. Rev.* **132**, 124 (1963).

²³H. G. Drickamer, R. W. Lynch, R. L. Clendenen, and E. A. Perez-Alburene, *Solid State Phys.* **19**, 135 (1966).

²⁴N. N. Roy and E. G. Steward, *Nature (London)* **224**, 905 (1969).

Flow of ³He-B through Narrow Channels

M. T. Manninen and J. P. Pekola

Low Temperature Laboratory, Helsinki University of Technology, SF-02150 Espoo 15, Finland

(Received 22 December 1981)

The critical current J_c of superfluid ³He-B through 0.8- μ m-diam channels has been measured. For small currents the pressure difference $\Delta P = 0$ along the flow channels within the resolution, implying small or zero dissipation. ΔP grows rapidly with increasing current above J_c ; a clear transition to dissipative flow is thus observed. The temperature dependence of J_c indicates that the superfluid density and the critical temperature are reduced inside the narrow flow channels.

PACS numbers: 67.50.Fi

The most important feature of a simple superfluid is that it can sustain mass flow without friction. At some critical current J_c , however, the superfluid state becomes unstable, which leads

to dissipation. This model was derived from experiments on He II; its validity in the case of ³He-B is currently of considerable interest. Parpia and Reppy¹ have observed the onset of